Development 134, 3593-3601 (2007) doi:10.1242/dev.011510

The *HECATE* genes regulate female reproductive tract development in *Arabidopsis thaliana*

Kristina Gremski, Gary Ditta and Martin F. Yanofsky*

Successful fertilization in plants requires the properly coordinated development of female reproductive tissues, including stigma, style, septum and transmitting tract. We have identified three closely related genes, *HECATE1* (*HEC1*), *HECATE2* (*HEC2*) and *HECATE3* (*HEC3*), the expression domains of which encompass these regions of the *Arabidopsis* gynoecium. The *HEC* genes encode putative basic helix-loop-helix (bHLH) transcription factors with overlapping functionality. Depending on the amount of *HEC* function missing, plants exhibit varying degrees of infertility, defects in septum, transmitting tract and stigma development and impaired pollen tube growth. The observed phenotypes are similar to those reported for mutations in the *SPATULA* (*SPT*) gene, which also encodes a bHLH transcription factor required for development of the same female tissues. We show that the HEC proteins can dimerize with SPT in a yeast two-hybrid system, indicating that the *HEC* genes work in concert with *SPT* to coordinately regulate development of the female reproductive tract. Furthermore, when the *HEC* genes are ectopically expressed from the CaMV 35S promoter, some of the resulting transgenic plants show pin-shaped inflorescences, suggesting that the *HEC* genes are probably involved in auxin-mediated control of gynoecium patterning.

KEY WORDS: *Arabidopsis*, Development, Stigma, Transmitting tract, Pollen tube growth

INTRODUCTION

The *Arabidopsis* gynoecium is a complex organ specialized for seed production and dispersal. It arises from two congenitally fused carpels and at maturity consists of an apical stigma for pollen capture, a short intervening style and a large central ovary where ovule and seed development occurs (Fig. 1A,B). The ovary is divided into two compartments by the septum. A specialized tissue called the transmitting tract, crucial for pollen tube growth, develops in the center of both the style and the septum.

During fertilization, pollen grains germinate on the stigma and grow downward through the stigma and transmitting tract before diverging laterally toward the ovules. Transmitting tract cells facilitate pollen tube growth by secreting a complex extracellular matrix (ECM) rich in acidic polysaccharides, and by undergoing a program of developmentally controlled cell death (Lennon et al., 1998; Wang et al., 1996; Crawford et al., 2007). A number of mechanisms involving chemical gradients and/or signal molecules have been proposed, whereby pollen tubes are guided from the stigma into the transmitting tract and out of the transmitting tract towards the awaiting ovules (Johnson and Preuss, 2002; Palanivelu et al., 2003; Palanivelu and Preuss, 2006). In the absence of proper transmitting tract differentiation, pollen tube growth is limited and fertility is reduced (Crawford et al., 2007).

Since proper development of female reproductive tissue is essential to the reproductive success of the plant, this process is likely to be highly regulated. A number of genes have been identified as important for patterning the stigma, style, septum and transmitting tract. These include *SPATULA* (*SPT*), *STYLISH1* (*STY1*), *STYLISH2* (*STY2*) and *ETTIN* (*ETT*). *SPT* encodes a basic helix-loop-helix (bHLH) transcription factor expressed early in septum and stigma development. Loss of *SPT* function leads to defects in septum and apical carpel fusion, loss of transmitting tract and a decrease in stigmatic tissue development (Alvarez and Smyth, 2002; Heisler et al., 2001). *STY1* and *STY2* encode RING-finger proteins that function in the development of the style (Kuusk et al., 2002; Sohlberg et al., 2006). *spt* mutants are epistatic to *sty1* mutants, suggesting that *SPT* and *STY* act in the same pathway (Sohlberg et al., 2006). *ETT*, which encodes an auxin-response factor (ARF), has been shown to restrict the expression domain of *SPT*. In *ett* mutants, transmitting tract tissue develops on the outside of the gynoecium, and removing *SPT* function from *ett* mutants rescues this defect (Heisler et al., 2001).

Previous studies indicate that the hormone auxin plays an important role in controlling development of the gynoecium. High levels of auxin have been postulated to accumulate in the style and form a gradient downward through the gynoecium (Nemhauser et al., 2000). Treatment of wild-type gynoecia with the auxin transport inhibitor NPA produces enlarged stigmas and styles reminiscent of weak *ett* phenotypes. Furthermore, application of NPA to *spt* gynoecia partially restores gynoecium development, indicating that auxin is especially important in patterning the development of the female reproductive tract (Nemhauser et al., 2000).

In this work, we report three new genes that play an important role in the complex program of gynoecium development. *HEC1*, *HEC2* and *HEC3* encode closely related bHLH transcription factors with overlapping functionality. Loss of *HEC* function leads to defects in the development of the transmitting tract, septum and stigma and to a decrease in fertility. Conversely, overexpression of *HEC* genes causes both the production of ectopic stigmatic tissue and gain-of-function phenotypes implicating them as components of the auxin-signaling pathway. HEC proteins heterodimerize with SPT in a yeast two-hybrid system, suggesting that these proteins are likely to cooperatively interact in controlling development.

MATERIALS AND METHODS

Mutant plants

The *hec1* allele corresponds to the GABI-KAT line 297B10 (Rosso et al., 2003). It was genotyped using the gene-specific primers oKG156 (5′-ACCACAACAACACTTACCCTTTTC-3′) and oKG157 (5′-GTTCCA-

Section of Cell and Developmental Biology, University of California San Diego, La Jolla, CA 92093, USA.

*Author for correspondence (e-mail: marty@ucsd.edu)

Accepted 2 August 2007

CACCCTTTCATAACCACT-3′) to amplify a wild-type fragment and the T-DNA-specific primer (5′-CCCATTTGGACGTGAATGTAGACAC-3′; sequence provided by GABI-KAT) in combination with oKG156.

The *hec3* allele corresponds to the SALK_005294 line (Alonso et al., 2003). It was genotyped using primers C-X1 (5′-GTGCTATTTCGTGA-AGAGACAAGAGA-3′) and C-X4 (5′-TCCTAACAAACCCTTATTTC-GTATCCA-3′) to amplify a wild-type fragment and C-X4 in combination with the T-DNA-specific primer JMLB2 (5′-TTGGGTGATGGTTCACGT-AGTGGG-3′).

The *ett-7* allele was kindly provided by Patricia Zambryski (University of California, Berkeley, CA). The *spt-2* allele was kindly provided by David Smyth (Heisler et al., 2001).

Generation of transgenic plants

HEC2-RNAi lines were generated by amplifying a 180 bp fragment, using primers oKG93 (5′-GGGATCCTCTAATGAACATGATGATGC-3′) and oKG110 (5′-TTATCGATTAACCGGGTTGGTGGTGAGGCATG-3′) for the 5′-3′ orientation, and primers oKG94 (5′-CCTCGAGTCTAATGAA-CATGATGATGC-3′) and oKG91 (5′-GGGTACCCCGGGTTGGTGGT-GAGGCATG-3′) for the 3′-5′ orientation. Both fragments were cloned into the pHANNIBAL vector (Wesley et al., 2001) and the entire cassette was subsequently cloned into pART27 (Gleave, 1992) to generate KG154-1. Phenotypes were analyzed in the T1 generation.

The *HEC3* rescue construct was generated by amplifying a genomic fragment that included 2979 bp upstream of the translational start site and the coding region, using primers oKG121 (5′-CCGTCGACCTTCCCA-TGCCTTGTAATCAC-3′) and oKG256 (5′-TGTCGACCTAGATTAA-TTCTCCTACTC-3′). A *Sal*I fragment was cloned into pMX202 to generate KG153-7. KG153-7 was transformed into the *hec1 hec3* double mutant and phenotypes were analyzed in the T1 and T2 generations. In situ analysis was performed to confirm that the promoter was sufficient to drive both septum and funiculus expression.

The *HEC1p::HEC1:GUS* construct was generated by amplifying a genomic fragment that included 2972 bp upstream of the translational start and the coding region up to, but not including, the stop codon. The region was amplified using primers oKG117 (5′-CCGTCGACCACCCAACT-ACCAACTAAATG-3′) and oKG118 (5′-CCGTCGACTCTAAGAATC-TGTGCATTGCC-3′). A *Sal*I fragment was cloned into pBI101.1 to generate KG92-12.

The *HEC2p::GUS* construct was generated by amplifying a genomic fragment that included 3058 bp upstream of the translational start codon, using primers oKG119 (5′-GGGTCGACGAATACAGAGCACTTGTT-CAAG-3′) and oKG187 (5′-CAGATCTCCTCCTTTTTTGTGGAATT-TATAG-3′). A *Sal*I/*Bgl*II fragment was cloned into pBI101.1 to generate KG128-6.

The *HEC3p::GUS* construct was generated by amplifying a genomic fragment that included 2979 bp upstream of the translational start codon, using primers oKG121 (5′-CCGTCGACCTTCCCATGCCTTGT-AATCAC-3′) and oKG188 (5′-GGTCGACAATTTTTGTTTGTTTG-GTTCG-3′). A *Sal*I fragment was cloned into pBI101.1 to generate KG141-5.

To generate the overexpression lines, coding sequences were PCR amplified using Col genomic DNA as a template and cloned into the pCR2.1-TOPO vector. *HEC1* was amplified using primers oKG83 (5′-GGTCGACATCTTTCTCTATGGATTCTGAC-3′) and oKG84 (5′-CGG-ATCCCATCATCATCTAAGAATCTGTG-3′). A *Sal*I/*Bam*HI fragment was cut out of pCR2.1 and cloned into pBIN-JIT (Ferrandiz et al., 2000) to create KG72-4. *HEC2* was amplified using primers oKG89 (5′-CGTCGACA-AAAAGGAGGATGGATAACTC-3′) and oKG90 (5′-CCCCGGGCAT-CATCATCTAAGAATCTGTG-3′). A *Sal*I/*Sma*I fragment was cloned into pBIN-JIT to create pKG68-4. *HEC3* was amplified using primers oKG95 (5′-CGTCGACCCAAACAAACAAAAATTATGA-3′) and oKG96 (5′-CGGATCCCTTGTCTAGATTAATTCTCC-3′). A *Sal*I/*Bam*HI fragment was cloned into pBIN-JIT to create pKG80-22. In the pBIN-JIT vector, the coding sequences were placed under the control of a double repeat of the 35S promoter. Overexpression phenotypes were analyzed in the T1 and T2 generations.

The integrity of all constructs was confirmed by sequencing.

RT-PCR

RNA was isolated using the Qiagen RNeasy Plant Mini Kit. The reverse transcriptase reaction was performed using the Promega Reverse Transcription System. *HEC1* was amplified with primers oKG83 and oKG84. *HEC2* was amplified with primers oKG89 and oKG90. *HEC3* was amplified with primers oKG95 and oKG96. A *β-TUBULIN* control amplification was performed using primers (5′-GGACAAGCTGGGAT-CCAGG-3′) and N-1137 (5′-CGTCTCCACCTTCAGCACC-3′). The annealing temperature was 58°C. The PCR amplification in Fig. S2A,B (see Fig. S2A,B in the supplementary material) was carried out using 2 μl of reverse transcriptase reaction, the *HEC* amplification was performed with 35 cycles, and *TUBULIN* was amplified using 25 cycles. In the PCR amplification shown in Fig. S2C (see Fig. S2C in the supplementary material), *HEC2* was amplified with 30 cycles using 1 μl of reverse transcriptase reaction, *SPT* was amplified with 28 cycles using 1 μl of reverse transcriptase reaction, and *TUB* was amplified with 25 cycles using 0.5 μl of reverse transcriptase reaction.

In situ hybridization

In situ hybridization was performed as described by Dinneny et al. (Dinneny et al., 2004). An antisense *HEC1* probe was transcribed with T7 polymerase (Promega) using a full-length coding sequence in pCR2.1 (KG62-1) that had been linearized with *Hin*dIII. An antisense *HEC2* probe was transcribed with T7 polymerase using a full-length coding sequence in pBluescript (KG100-1) linearized with *Spe*I. An antisense *HEC3* probe was transcribed with T7 polymerase using a full-length coding sequence in pCR2.1 (KG76-2) linearized with *Spe*I.

Microscopy and histology

Staining for β-glucuronidase expression was as described (Blázquez et al., 1997) with minor modifications. Wild-type (Columbia ecotype) and transgenic fruit and flowers were fixed and analyzed by scanning electron microscopy as previously described (Liljegren et al., 2000).

Aniline Blue staining for pollen tubes was performed after emasculating flowers just prior to pollination (late stage 12), growing them for another 18-24 hours to allow transmitting tract and ovule development to be completed, and then hand-pollinating them maximally. After allowing another 24 hours for pollen growth, they were fixed, cleared, stained with Aniline Blue (Jiang et al., 2005) and examined under a fluorescence microscope.

Staining with Alcian Blue 8GX was used to visualize the transmitting tract. Alcian Blue stains the acidic mucopolysaccharide component of the transmitting tract ECM (Scott and Dorling, 1965). Paraplast-embedded flowers and inflorescences were sectioned at 4 μm and fixed to slides. Slides were then de-waxed with Histoclear (National Diagnostics), rehydrated through a gradual ethanol series, counterstained for 5 minutes with 0.1% Nuclear Fast Red, rinsed, stained for 5 minutes with Alcian Blue pH 3.1, rinsed again, dried briefly at 37°C, then mounted directly in Permount (Fischer Scientific).

Yeast two-hybrid system

Directed yeast two-hybrid interactions were conducted as described (Pelaz et al., 2001). Full-length *HEC1* was cloned into both the bait vector pBI-880 to make SP7-2 and into the prey vector pBI-771 to make SP18. Full-length *HEC2* was cloned into both the bait vector pBI-880 to make SP8-4 and into the prey vector pBI-771 to make SP19. Full-length *HEC3* was cloned into the prey vector pBI-771 to make SP20. The full-length *HEC3* in the bait vector was able to activate the reporters on its own. Hence, a partial *HEC3* fragment, which included amino acids 92-224, was cloned into pBI-880 to make SP14-1. The SPT prey vector had previously been isolated from a cDNA library in a yeast two-hybrid screen with IND. The partial clone contains amino acids 47-373.

RESULTS

Identification of the *HECATE* (*HEC*) genes

Previous work identified the bHLH transcription factor INDEHISCENT (IND) as a key regulator of valve margin development in the *Arabidopsis* fruit (Liljegren et al., 2004).

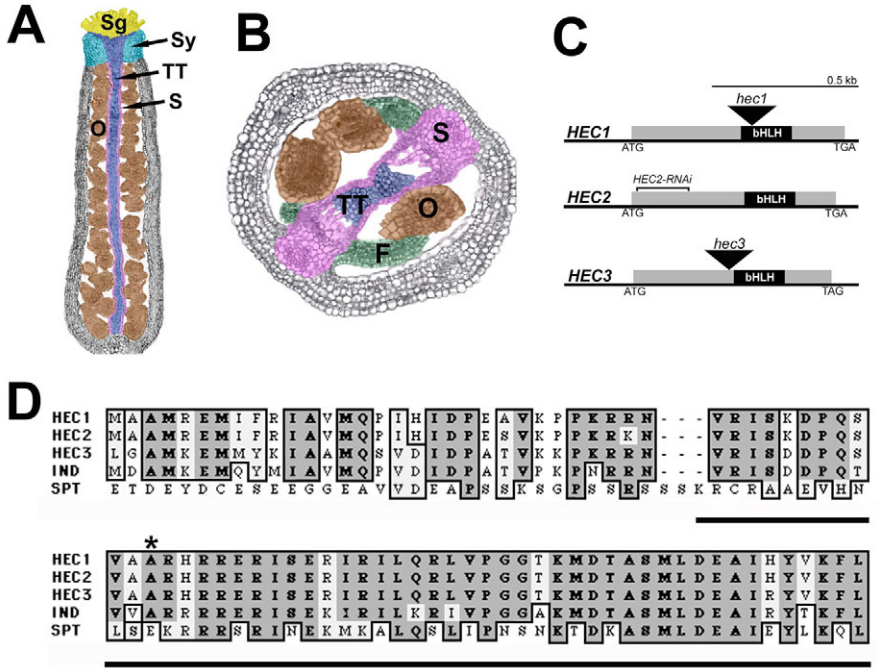

Fig. 1. Fruit tissue structure and the *HECATE* genes of *Arabidopsis*. (**A**,**B**) Colorized longitudinal (A) and transverse (B) sections showing internal fruit tissues of wild-type *Arabidopsis*. Stigma (Sg), yellow; style (Sy), turquoise; septum (S), pink; transmitting tract (TT), blue; ovules (O), brown; ovule funiculus (F), green. (**C**) Diagrams of *HEC1* (At5g67060), *HEC2* (At3g50330) and *HEC3* (At5g09750) showing the location of the bHLH domain. Positions of the T-DNA (not shown to scale) insertions in *HEC1* and *HEC3* are represented by triangles. The region of *HEC2* used for creating the *HEC2-RNAi* construct is bracketed. (**D**) Alignment of the bHLH domains (underlined) of the HEC, INDEHISCENT (IND) (Liljegren et al., 2004) and the distantly related SPATULA (SPT) (Heisler et al., 2001) proteins. The alignment includes a region upstream of the bHLH domain, where the HECs and IND also show conservation. The asterisk marks an alanine that replaces the conserved glutamate carried by most other *Arabidopsis* bHLH proteins.

Reasoning that bHLH proteins related to IND might also function in plant development, we performed a BLAST search to find those genes most closely related to *IND*. *HEC1* (At5g67060; BHLH088), *HEC2* (At3g50330; BHLH037) and *HEC3* (At5g09750; BHLH043) were thus identified. All three *HEC* genes were subsequently found to function in gynoecium development, but to have roles distinct from that of *IND*.

Like *IND*, each of the *HEC*s is composed of a single small exon (Fig. 1C). *HEC1*, *HEC2* and *HEC3* encode proteins of 242, 232 and 225 amino acids, respectively. The *IND* and *HEC* gene products share extensive protein sequence similarity in the bHLH domain, as well as in a 30 amino acid N-terminal extension of this region (Fig. 1D). Similarity in this 30 amino acid region leads to both IND and HECs being grouped as a subfamily of bHLH proteins (Heim et al., 2003). HEC1 and HEC2 are the most closely related and share 61% amino acid identity across the length of the proteins and 100% identity within the bHLH domain. Previous phylogenetic analysis of the *Arabidopsis* bHLH transcription factor family placed *HEC1* and *HEC2* in regions that arose from a putative interchromosomal duplication event (Toledo-Ortiz et al., 2003). Protein alignment of the HECs with IND and more-distantly related bHLH factors reveals that the HECs, like IND, lack a conserved glutamate at position 13 of the basic domain (Fig. 1D, asterisk). This glutamate has been shown to be important for DNA binding (Ellenberger et al., 1994; Ma et al., 1994). Thus, if the HECs regulate gene transcription through DNA binding, they are likely to do so through the use of other residues.

The *HEC* genes are expressed in the developing septum, transmitting tract and stigma

To investigate whether the *HEC* genes function in gynoecium development, we analyzed their expression patterns using both RNA in situ hybridization and β-glucuronidase (GUS) reporter gene constructs. In contrast to the valve margin expression pattern described for *IND* (Liljegren et al., 2004), all three *HEC* genes were found to be expressed in the stigma and septum during stages 8 to 12 of flower development.

RNA in situ analysis showed that for all three *HEC*s, expression was first observed during stage 8 of gynoecium development, in the medial ridges of the septum, which have grown together and fused at this time (Fig. 2A-C, large arrowheads), and in the apical tips (Fig. 2G, lower arrow), where the stigma will arise. By stage 10 to early stage 12, hybridization signal was localized to the transmitting tract (Fig. 2D-H, large arrowheads) and developing stigmas (Fig. 2G,H, arrows). Patchy signal was also apparent in the ovules for *HEC1* and *HEC2* (Fig. 2D-E, small double arrowheads) and in the ovule funiculus for *HEC3* (Fig. 2F, arrow). By late stage 12, just prior to fertilization, *HEC3* expression was still evident in the transmitting tract (Fig. 2I,J, large arrowheads) and was strong in the ovule funiculus (small arrowheads), but was no longer visible in the stigma (arrow). *HEC1* and *HEC2* expression could no longer be detected by late stage 12 (data not shown).

GUS reporter results confirmed the septum and stigma expression of *HEC1* and *HEC2* (see Fig. S1A-D in the supplementary material) and also indicated that *HEC3* funiculus expression continued even after pollination (see Fig. S1E in the supplementary material, arrowheads). Some *HEC2p::GUS* lines also expressed GUS in pollen and the nectaries (data not shown), and a number of the *HEC3p::GUS* lines showed expression in vasculature (see Fig. S1E in the supplementary material, arrow). GUS analysis did not confirm *HEC3* transmitting tract and stigma expression, *HEC1* and *HEC2* ovule expression, or *HEC1* anther expression, presumably because the GUS constructs lack essential DNA regulatory elements necessary for them to represent the entire pattern of expression indicated by RNA in situ hybridization.

The close sequence similarity of the *HEC* genes and their overlapping expression patterns suggest that they might have partially redundant functions in stigma and septum development.

hec1 and *hec3* mutations reduce fertility

To determine the functions of the *HEC* genes, we identified T-DNA insertion lines in *HEC1* and *HEC3* from available mutant collections (Fig. 1C) and confirmed these lines as RNA-nulls by RT-PCR (see Fig. S2A,B in the supplementary material). An absence of *HEC3*

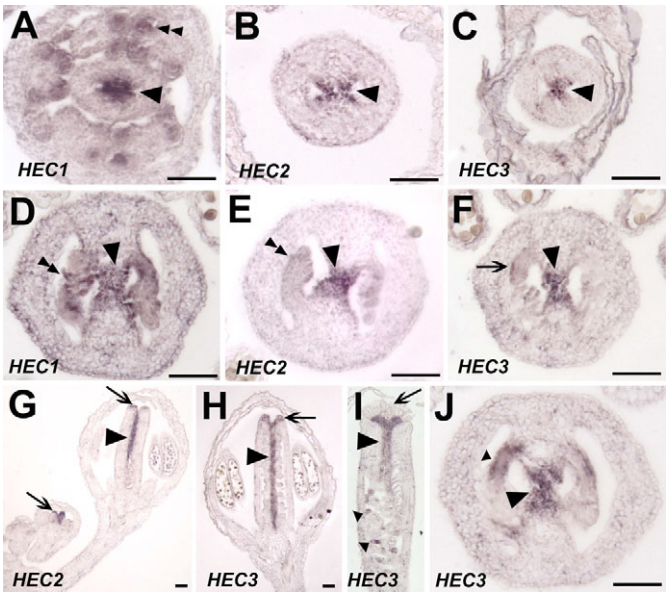

Fig. 2. RNA in situ analysis of *HEC* expression during gynoecium development in *Arabidopsis*. (**A-C**) Transverse sections through stage 8 gynoecia. *HEC1*, *HEC2* and *HEC3* are expressed in the developing septum (arrowheads). The *HEC1* signal seen in the anthers at this stage (double arrowhead) was not seen for *HEC2* or *HEC3* and was not duplicated by the *HEC1 GUS* reporter (see Fig. S1E in the supplementary material). (**D-F**) Transverse sections through early stage 12 gynoecia. *HEC1*, *HEC2* and *HEC3* expression becomes localized to the developing transmitting tract (arrowheads). *HEC1* and *HEC2* are expressed in ovules (small double arrowheads) and *HEC3* shows expression in the ovule funiculus (arrow). (**G**,**H**) Longitudinal sections through stage 8 and stage 11 flowers. *HEC1* (G) and *HEC3* (H) expression is evident in the developing septum and transmitting tract (arrowheads) and stigma (arrows). (**I**,**J**) Longitudinal and transverse sections through late stage 12 gynoecia. *HEC3* continues to be strongly expressed in the transmitting tract (large arrowheads) and ovule funiculus (small arrowheads), but not in the stigma (arrow). *HEC1* and *HEC2* expression can no longer be detected at this time (data not shown). Scale bars: 50 μm.

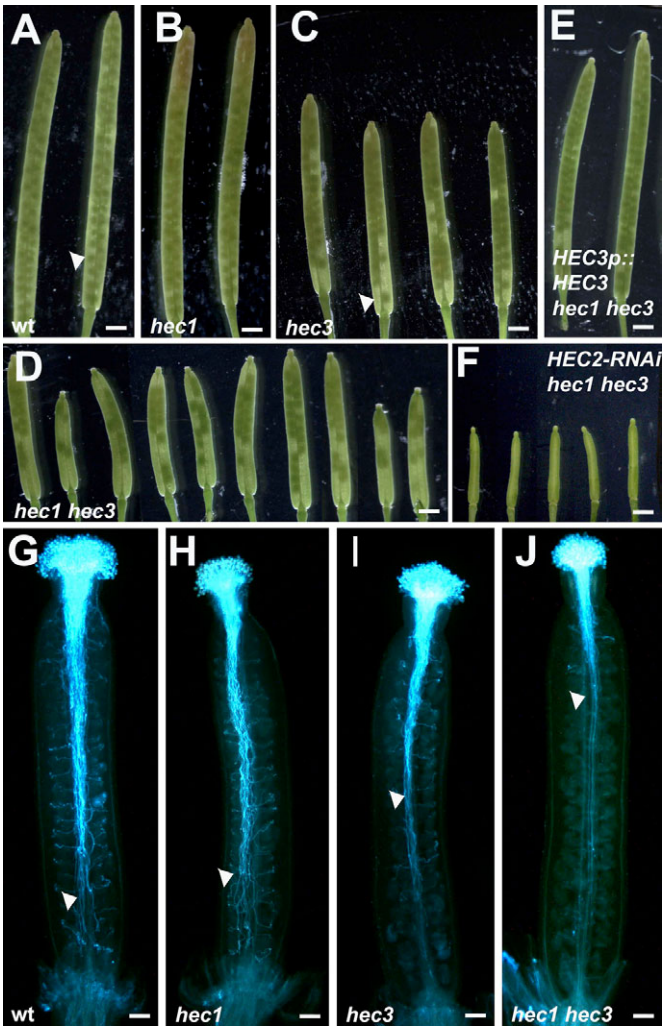

Fig. 3. Mutations in *Arabidopsis HEC* genes result in reduced fertility. (**A**) Wild-type Col-0 fruit; arrowhead points to shadow cast by developing seed. (**B**) *hec1* fruit show no obvious abnormal phenotype. (**C**) *hec3* fruit are shorter and exhibit reduced fertility; arrowhead points to empty space that should be occupied by seed. (**D**) *hec1 hec3* fruit are variable in size but generally short, with significantly reduced fertility. (**E**) *HEC3p:HEC3* rescues *hec1 hec3*. (**F**) *HEC2-RNAi hec1 hec3* fruit are completely sterile. (**G-J**) Pollen tubes stained with Aniline Blue 24 hours post-pollination. In the wild type (G) and *hec1* (H), the bulk of the pollen tubes have nearly reached the base of the ovary (arrowhead). In *hec3* (I), pollen tubes are fewer in number and have not penetrated as far as in the wild type or *hec1* (arrowhead). In *hec1 hec3* (J) there is a significant reduction in pollen tubes entering the ovary, and penetration along the apical-basal axis is greatly diminished (arrowhead). Scale bars: 1 mm in A-F; 0.1 mm in G-J.

RNA in the *hec3* mutant was further demonstrated by in situ hybridization (data not shown). No satisfactory mutants in *HEC2* were available at the time of this work.

hec1 mutant plants showed no alteration in fruit phenotype (Fig. 3A,B; Table 1). *hec3* mutant plants had smaller fruit and a modest reduction in fertility compared with wild type (59% wild-type seed set) (Fig. 3A,C; Table 1). Reciprocal crosses revealed the fertility defect to be female-specific (data not shown). The *hec1 hec3* double mutant had a sizable reduction in overall fertility (17% wild-type seed set), along with significant variations in individual fruit size and seed yield (Fig. 3A,D; Table 1). Seed distribution was biased toward the apical half of the carpel, but substantial fertilization also occurred in the basal half (Fig. 3D). The fact that the double mutant had a more severe phenotype than either single mutant demonstrates that both genes are required for wild-type levels of fertility.

We were able to rescue the fertility defect of *hec1 hec3* plants to approximately wild-type levels by transforming them with a *HEC3* rescue construct composed of 3 kb of the *HEC3* promoter driving the *HEC3* coding region (Fig. 3E). This result would be anticipated as the *hec1* mutation alone produces no obvious change in the fruit, and it confirms that the observed mutant phenotypes are due to the *hec1* and *hec3* mutations.

Defects in pollen tube growth in the *hec* mutants

Stigma and transmitting tract provide the apical-to-basal tissue path for pollen tube growth in *Arabidopsis*. Since the *HEC* genes are expressed in these tissues, it seemed likely that the loss of fertility in *hec* mutants would correlate with aberrant or reduced pollen tube growth. To visualize pollen tubes within the ovary, we used an

Table 1. Loss of *HEC* function leads to a reduction in fertility

Genotype	Seeds/fruit (*n*)*	% seed set
Wild type	50.9±3.9 (78)	100
hec1	50.1±8.9 (77)	98
hec3	29.9±7.3 (80)	59
hec1 hec3	8.4±3.8 (78)	17

*The average number of seeds per fruit plus or minus the standard deviation (*n*=the number of fruits sampled). Fruits were collected from the primary shoot of five plants per genotype, starting at fruit number five, and going up to fruit number twenty.

Aniline Blue staining technique (Jiang et al., 2005) 24 hours after hand-pollinating emasculated carpels (Materials and methods). Aniline Blue stains callose, a component of pollen tubes, allowing them to be visualized by fluorescence microscopy.

Wild-type and *hec1* gynoecia showed an abundance of pollen tubes throughout the length of the transmitting tract (Fig. 3G,H). Fertilization events, evident as lateral deviations in tube growth, likewise occurred throughout the entire length of the ovary. *hec3* carpels showed significantly fewer pollen tubes and pollination events, particularly in the basal half of the gynoecium (Fig. 3I). This difference was even more pronounced for the *hec1 hec3* double mutant (Fig. 3J). A similar pattern of reduced pollen tube growth was found when carpels were examined only 6 to 7 hours after pollination, when wild-type pollen tubes had not yet reached the bottom of the ovary (data not shown).

HEC1 and *HEC3* are necessary for stigma and transmitting tract development

Both stigma and style showed obvious developmental abnormalities in *hec* mutants. Compared with wild type (Fig. 4K), stigmas were smaller and more variable in size in *hec1 hec3* mutants (Fig. 4L). Although not evident in Fig. 4, there was also a slight tendency for the style to be somewhat longer in the double mutant. To visualize the transmitting tract in *hec* mutants, post-fertilization flowers were thin-sectioned and stained with Alcian Blue, a dye that detects acidic polysaccharides characteristic of the transmitting tract ECM. Wild type showed a characteristically large, intensely staining transmitting tract (Fig. 4A,H, arrowheads). The transmitting tract of *hec1* was indistinguishable from that of wild type in size, staining intensity and cytology (Fig. 4B). The *hec3* transmitting tract was smaller in size than wild type in both the septum and the style (Fig. 4C,I), but had the same general appearance as wild type. The *hec1 hec3* double mutant, however, had dramatically reduced Alcian Blue staining in both the style and the septum compared with wild type (Fig. 4D,E,J). In analyzing pre-fertilization stages of development, we found that the transmitting tract of the *hec1 hec3* double mutant had no delay in onset of ECM production, but produced less ECM than wild type (see Fig. S3 in the supplementary material). Taken together, these data demonstrate that *HEC1* and *HEC3* are redundantly required for transmitting tract differentiation.

Reducing *HEC2* RNA levels in the *hec1 hec3* double mutant intensifies defects in stigma and septum development

Given the sequence similarity and overlapping expression domains among the *HEC* genes, and considering the synergistic nature of *hec1* and *hec3* single mutations, it seemed likely that all three *HEC* genes would share functionally related roles in *Arabidopsis*. To confirm this hypothesis and to substantiate a role for *HEC2* in gynoecium development, we used RNAi to create the equivalent of a *hec1 hec2 hec3* triple mutant. To make the RNAi construct we used

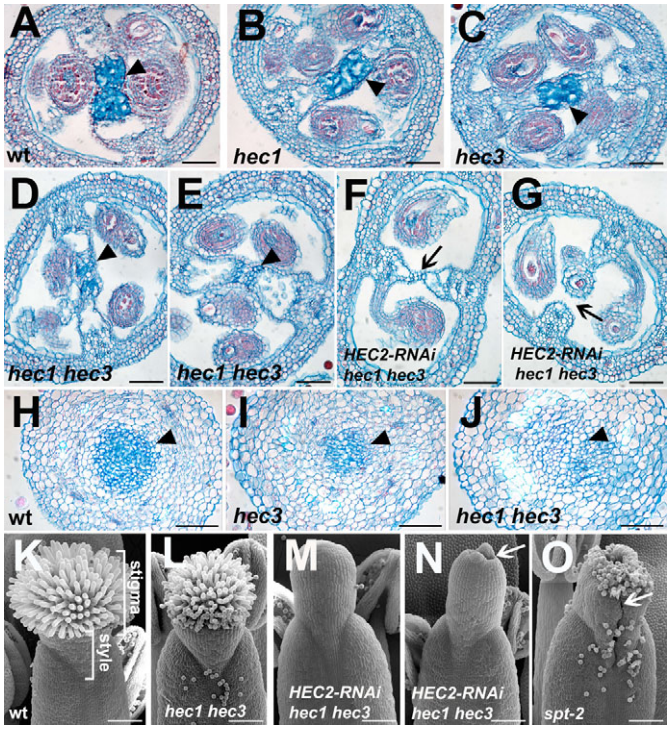

Fig. 4. Loss of transmitting tract and stigma development in *hec* mutants. (**A-G**) Transverse sections of stage 14 *Arabidopsis* ovaries stained with Alcian Blue to reveal the transmitting tract (arrowheads) and with Fast Red as a counterstain. In the wild-type (Col-0) gynoecium (A), the ECM of the transmitting tract stains bright blue in the center of the septum. The *hec1* transmitting tract (B) is essentially equivalent to wild type, but the *hec3* transmitting tract (C) is noticeably smaller. Typical examples of *hec1 hec3* transmitting tracts (D,E) are severely reduced in size within narrowed septa. Typical examples of *HEC2-RNAi hec1 hec3* gynoecia (F,G) exhibit no blue staining at the transmitting tract, and have either only a few cells at the septum fusion point (F, arrow) or an unfused septum (G, arrow). (**H-J**) Transverse sections of stage 14 styles stained with Alcian Blue and Fast Red. The transmitting tract (arrowhead) is reduced for *hec3* in the stylar region (I) in comparison with wild type (H). *hec1 hec3* has very little transmitting tract in the style (J). (**K-O**) Scanning electron micrographs of stigma and style regions of stage 14 gynoecia. The stigma of *hec1 hec3* gynoecia (L) are significantly less well developed than those of wild-type Col-0 (K). *HEC2-RNAi hec1 hec3* gynoecia (M,N) lack any stigmatic development and have longer styles than wild type. Some fruit displayed a defect in apical fusion (N, arrow) similar to that of *spt-2* (O, arrow; Ler background). Scale bars: 50 μm in A-J; 100 μm in K-O.

180 bp from the 5′ coding region of *HEC2* (Fig. 1C). This region contains some areas of close sequence similarity to *HEC1*, but little similarity to *HEC3*. The construct was transformed into both the wild type and the *hec1 hec3* double mutant.

RT-PCR analysis of several independent lines of *HEC2-RNAi* in the wild type revealed a strong to moderate reduction in the level of both *HEC1* and *HEC2* RNA and only a slight effect on *HEC3* RNA (see Fig. S2C,D in the supplementary material). These *HEC2-RNAi* lines, equivalent to *hec1 hec2* double mutants, showed little or no effect on fertility (data not shown). However, when the *HEC2-RNAi* construct was transformed into the *hec1 hec3* double mutant, 8 of 32 lines exhibited complete sterility (Fig. 3F). Such lines had dramatic defects in apical gynoecium development, with a complete absence of stigmatic tissue and, in many cases, an incomplete fusion of the

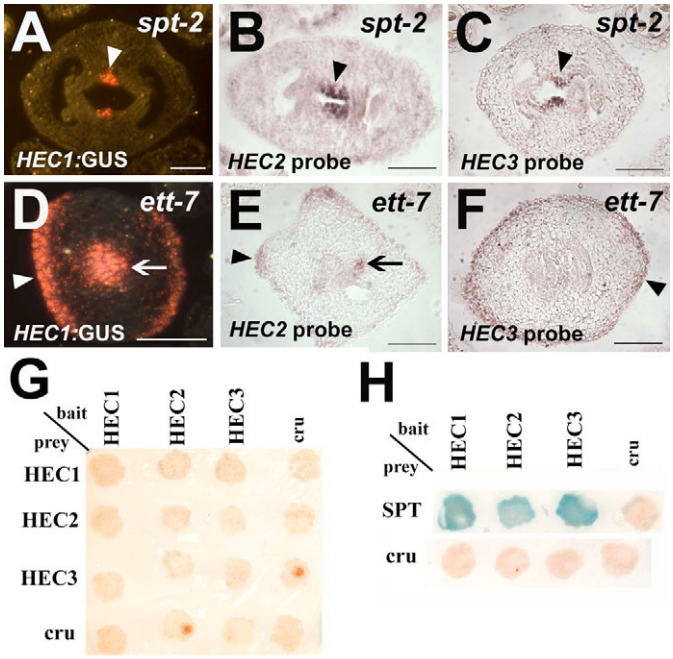

Fig. 5. The *Arabidopsis* HECs interact with SPT in yeast and are negatively regulated by ETT. (**A-C**) The HECs are still expressed (arrowheads) in the septum in the *spt-2* mutant. *HEC1* expression (A) was analyzed by crossing the *HEC1p:HEC1:GUS* line into *spt-2*, and *HEC2* (B) and *HEC3* (C) expression was analyzed directly by in situ hybridization. (**D-F**) The *HEC*s are ectopically expressed in abaxial cell layers of the gynoecium (arrowheads) in *ett-7*. *HEC1* expression (D) was analyzed by crossing the *HEC1p:HEC1:GUS* line into *spt-2*, and *HEC2* (E) and *HEC3* (F) expression was analyzed directly by in situ hybridization. Expression could also still be seen in the septum (arrows) for *HEC1* (D) and *HEC2* (E). (**G**) The HEC proteins do not homodimerize or heterodimerize with each other in a yeast two-hybrid system. Full-length HEC1 and HEC2 were used in both the bait and prey constructs. Full-length HEC3 was used as prey. However, an N-terminal deletion of HEC3 was used as the bait, as the full-length HEC3 bait construct activated the yeast reporter genes on its own (data not shown). The protein cruciferin was used as a negative control. Results were confirmed with the HIS3 reporter. (**H**) The HEC proteins form heterodimers with SPT in a yeast two-hybrid system. An N-terminal deletion of SPT was used as the prey construct (see Materials and methods). The protein cruciferin was used as a negative control. Results were confirmed with the HIS3 reporter. Scale bars: 50 μm.

apical region of the style (Fig. 4M,N). The style of *HEC2-RNAi hec1 hec3* plants was exceptionally long. We found severe effects on septum and transmitting tract development in *HEC2-RNAi hec1 hec3* gynoecia (Fig. 4F,G). The septum was either unfused (Fig. 4G, arrow) or had only a few cells at its thinnest point (Fig. 4F, arrow). Alcian Blue staining of the transmitting tract was never observed. Since this phenotype is reminiscent of that reported for mutants of *SPT* (see below), we specifically confirmed that there was no reduction in *SPT* RNA in the *HEC2-RNAi hec1 hec3* lines (see Fig. S2C in the supplementary material). We also confirmed that the fertility defect of *HEC2-RNAi hec1 hec3* lines was female-specific by crossing *HEC2-RNAi hec1 hec3* pollen onto wild-type flowers. These crosses resulted in fruit of normal length (data not shown).

Individual *HEC2-RNAi hec1 hec3* lines are formally equivalent to *hec1 hec2 hec3* triple mutants. The severe developmental defects seen in these lines indicate that the *HEC* genes are functionally redundant and play a fundamental role in stigma and transmitting tract development and in the post-genital fusion of the septum and the apical gynoecium. Owing to the requirement of the three *HEC* genes for female fertility, we named them after the Greek goddess of fertility Hecate, often portrayed as three women.

Interactions between *SPATULA* and the *HECs*

The well-studied developmental regulator *SPATULA* (*SPT*) encodes a bHLH protein that is considerably larger than any of the HEC proteins (373 amino acids versus approximately 230 amino acids) and is poorly conserved with the HEC proteins (Fig. 1D). Nevertheless, *SPT* is expressed in both septum and stigma during stages 6 to 11 (Heisler et al., 2001), and genetic studies have shown it to be required for septum, transmitting tract and stigma formation (Alvarez and Smyth, 2002). We therefore investigated possible interactions between *SPT* and the *HEC*s.

Since *SPT* expression is detectable at earlier stages of gynoecium development than is *HEC* expression (Heisler et al., 2001), the possibility existed that *SPT* might be a transcriptional regulator of the *HEC*s. We examined this by analyzing the expression of *HEC1*, *HEC2* and *HEC3* in early carpels of plants carrying the strong *spt-2* allele (Fig. 5A-C). All three *HECs* continued to be expressed in this mutant background, indicating that a functional SPT protein is not required for *HEC* gene expression.

A more likely possibility was that the SPT and HEC proteins might interact cooperatively to regulate development. bHLH proteins are known to both homodimerize and heterodimerize, and dimer formation is essential for transcriptional regulation (Murre et al., 1994; Massari and Murre, 2000). We therefore used a yeast two-hybrid system to investigate protein-protein interactions among the *HEC1*, *HEC2*, *HEC3* and *SPT* gene products. The HEC proteins do not form either homodimers or heterodimers in yeast, but each is capable of heterodimerizing with SPT (Fig. 5G,H). If the HEC proteins function as transcriptional regulators, the data strongly suggest that SPT is likely to be a required partner.

ETTIN is a negative regulator of *HEC* gene expression

Since both *SPT* and the *HEC* genes are required for aspects of interior carpel development, specifically septum and transmitting tract development, it is relevant that mutants in the ARF factor *ETT* display a dramatic phenotype in which transmitting tract tissue develops on the outside of the gynoecium. This externalization of transmitting tract derives at least in part from the unrestricted expression of *SPT* in carpel valves (Heisler et al., 2001). We wanted to determine whether the *HEC* genes might also be under *ETT* control and play a similar role in the formation of external ectopic transmitting tract in *ett* mutants. *HEC* expression was examined in *ett-7* gynoecia and found to be equivalent to that seen for *SPT*. The *HEC*s were ectopically expressed on the outside of *ett-7* gynoecia (Fig. 5D-F). *ETT* therefore negatively regulates *HEC* expression in the abaxial gynoecium in a similar manner as it does *SPT*.

Overexpression of the *HEC* genes produces ectopic stigmatic tissue, *ett*-like and *pin*-like phenotypes

To further examine the effects of ectopic *HEC* activity, we generated overexpression lines in which *HEC* gene expression was driven from the constitutive 35S promoter. Overexpression of each *HEC* gene resulted in flowers that produced ectopic carpelloid tissue, most often stigmatic tissue (Fig. 6B,C,D, arrowheads; Fig. 6B,C, insets). The data indicate that the *HEC* genes are able to activate carpel identity factors when ectopically expressed.

The overexpression of *HEC1* and *HEC3* also occasionally led to the production of gynoecia with defects in apical-basal polarity reminiscent of a weak *ett* phenotype. Carpels had enlarged stigmas, reduced ovaries and elongated gynophores (Fig. 6G-I). The *HEC* genes thus could be involved in the *ETT*-mediated auxin-signaling pathway needed for apical-basal development. This possibility is further supported by even more extreme phenotypes seen among overexpressing lines, such as those shown in Fig. 6K,L. Here, pin-shaped inflorescences or carpelloid stalks were observed, resembling those that result from loss of the auxin efflux carrier *PIN-FORMED1* (*PIN1*) or from treatment with the chemical NPA, an auxin transport inhibitor (Okada et al., 1991). These dramatic phenotypes suggest that in these *35S::HEC1* and *35S::HEC3* lines there was an alteration of auxin levels, auxin transport and/or auxin perception.

DISCUSSION

The role of the *HECATE* genes in the development of the transmitting tract and stigma

Pollen tubes must travel through several distinct tissues before reaching ovules, including the stigma, the stylar transmitting tract and the septum transmitting tract. Coordinated development of these tissues is crucial for successful fertilization. We report here the identification of three related bHLH transcription factors, HEC1, HEC2 and HEC3, that are required for this process. All three genes share some degree of functional equivalency as shown by the synergistic effect of deficiencies in each. Whereas no abnormal phenotype was observed with an RNA-null mutation in *HEC1*, an RNA-null mutant of *HEC3* displayed a moderate loss of fertility and decreased transmitting tract tissue in both septum and style. A *hec1 hec3* double mutant displayed substantial defects in both fertility and transmitting tract development. The development of stigmatic tissue was reduced and there was a slight increase in the size of the style. To examine a possible contribution of *HEC2* toward the development of female reproductive tissues, we created a *HEC2-RNAi* construct and introduced it into the *hec1 hec3* background, establishing the equivalent of a *hec1 hec2 hec3* triple mutant. Transgenic lines with the most-extreme phenotypes displayed a complete loss of fertility and severe defects in stigma and septum development. *HEC2-RNAi hec1 hec3* plants lacked any stigmatic or transmitting tract cells and frequently lacked both style and septum fusion. These results are consistent with the idea that all three *HEC* genes share some measure of functional redundancy. Overexpression studies support this contention. Overexpression of any of the individual *HECs* led to the ectopic production of stigmatic tissue, consistent with their requirement for stigma development.

The relationship between the HEC/IND subfamily and the SPT subfamily of bHLH transcription factors

The HEC proteins and the previously characterized valve margin specification factor IND (Liljegren et al., 2004) belong to an atypical group of bHLH transcription factors. Most *Arabidopsis* bHLH proteins are thought to have evolved from an ancestral group of bHLHs common to both plants and animals (group B) and contain a conserved glutamate in the basic region (Heim et al., 2003; Toledo-Ortiz et al., 2003). This glutamate contacts DNA at the bHLH recognition sequence, the E-box (Ellenberger et al., 1994). SPT contains this crucial glutamate, but the HECs and IND have an alanine substitution (Fig. 1D). Animal group-C bHLH proteins, which also lack the conserved glutamate, have been shown to bind DNA in combination with group-B bHLHs using a different recognition site (Bacsi et al., 1995; Swanson et al., 1995).

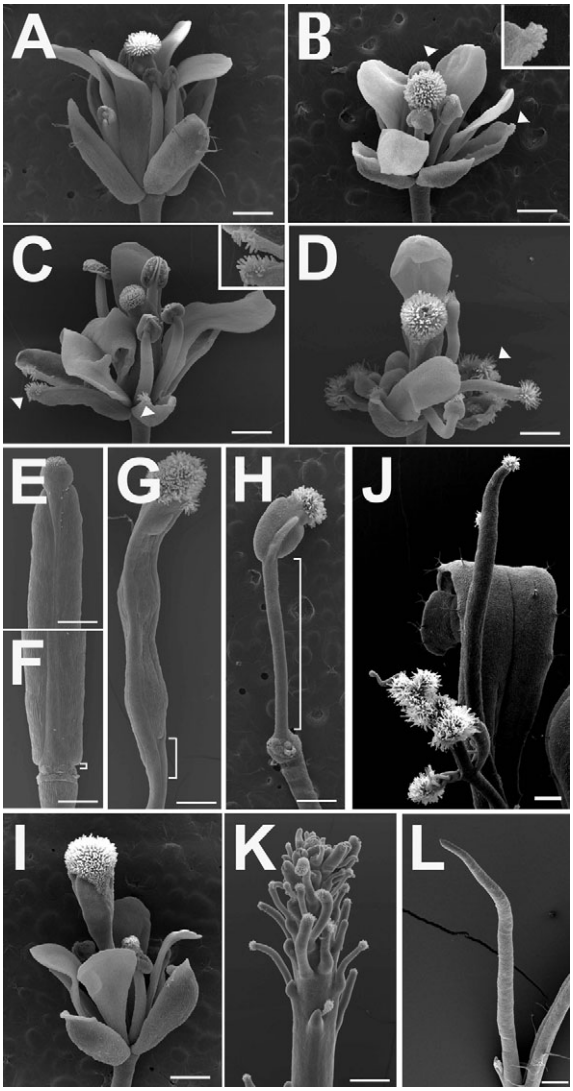

Fig. 6. Overexpression of *HEC* genes in *Arabidopsis*. (**A**) Wild-type flower. (**B**) *35S::HEC1* flower. Ectopic stigmatic tissue on anthers and sepals (arrowhead; inset shows an enlarged view of the region indicated by the lower arrowhead). (**C**) *35S::HEC2* flower. Ectopic stigmatic tissue on sepals (arrowheads; inset shows an enlarged view of the region indicated by the left arrowhead). (**D**) *35S::HEC3* flower. Most floral organs have carpelloid tissue (arrowhead). (**E**) Wild-type fruit (apical). (**F**) Wild-type fruit (basal). Gynophore is bracketed. (**G**) *35S::HEC3* fruit. Note the enlarged stigma, reduced ovary and elongated gynophore (bracketed). (**H**) *35S::HEC1* fruit. Note the enlarged stigma, reduced ovary and elongated gynophore (bracketed). (**I**) *35S::HEC1* flower. The gynoecium has an enlarged stigma, a reduced ovary and an elongated gynophore. (**J**) *35S::HEC1* inflorescence. Primary shoot terminates in a stigma. Axillary shoots form carpelloid structures with overproliferation of stigmatic tissue. (**K**) *35S::HEC3* inflorescence. Flowers transformed into carpelloid stalks capped by stigmas. (**L**) *35S::HEC1* inflorescence. No floral development. Scale bars: 400 μm.

In the current study, we investigated possible interactions between *SPT* and the *HEC*s. Because *SPT* is expressed at earlier stages of gynoecium development than the *HEC* genes (Heisler et al., 2001), the possibility existed that it might function as an upstream regulator of *HEC* expression. We therefore examined *HEC* expression in

plants carrying the strong *spt-2* allele and found that the *HEC* genes were still expressed, implying that *SPT* is not required for activation. We then considered the possibility that *SPT* and *HEC* gene products might interact with each other. This was shown to be the case. HEC proteins can form heterodimers with SPT in a yeast two-hybrid system, but cannot heterodimerize or homodimerize with each other. SPT can also heterodimerize with IND, the closest relative of the HECs (data not shown). Since SPT is expressed more widely during development than either the HECs or IND, but nevertheless encompasses the expression domains of both (Heisler et al., 2001), it seems likely that SPT and the HECs work in concert to carry out certain developmental programs and that SPT, because of its broader expression domain, interacts with yet other bHLH proteins to carry out additional developmental programs. It is relevant to note here that constitutive overexpression of *SPT* does not produce mutant phenotypes (M. Groszmann, PhD thesis, Monash University, 2005), as does overexpression of the *HEC*s. This observation is consistent with the possibility that the HECs are able to dimerize with broadly expressed proteins, whereas SPT requires partners with more limited expression domains.

Do the *HEC* genes play a role in the auxin-signaling pathway in the gynoecium?

A fundamental role has been suggested for the hormone auxin in patterning the *Arabidopsis* gynoecium, with high levels of auxin conferring apical tissue identity (stigma/style) and low levels of auxin leading to basal (gynophore) development (Nemhauser et al., 2000). The *ETT* gene is an important mediator of auxin effects. Mutations in *ETT* cause severe defects in gynoecium development, including an enlarged stigma, an elongated gynophore and a reduced ovary that develops transmitting tract tissue on the outside (Sessions and Zambryski, 1995). *SPT* is also likely to be involved in auxin patterning, both as a target of auxin regulation and as a mediator of auxin effects. *SPT* is ectopically expressed in the *ett* gynoecium, most notably in the inverted transmitting tract tissue on the outside of carpels (Heisler et al., 2001). Mutations in *SPT* can suppress mutations in *ETT* (Heisler et al., 2001). *spt-2* mutants can also be partially rescued by the auxin transport inhibitor NPA, and *spt-2* gynoecia are less sensitive than wild-type gynoecia to NPA effects on apical-basal patterning (Nemhauser et al., 2000).

If the HECs operate coordinately with SPT as protein partners, it is likely that both proteins are targets of auxin regulation and would be similarly affected by mutations in *ETT*. We found that all three *HEC* genes were, like *SPT*, ectopically expressed in external transmitting tract tissue in the *ett-7* mutant. The *HEC*s, like *SPT*, are therefore implicated as possible targets of auxin regulation.

The overexpression phenotype of the *HEC*s further suggests involvement in auxin patterning. Some of the phenotypes of *HEC*-overexpressing lines were similar to those of auxin-related mutants. *35S::HEC1*, *35S::HEC3* and, to a lesser degree, *35S::HEC2* lines occasionally produced gynoecia with defects in apical-basal patterning resembling those of a weak *ett* mutant (Fig. 6G-J; data not shown). Several independent *35S::HEC1* lines produced pin-shaped, flowerless inflorescences. We also observed stalk-like floral structures capped by stigmatic tissue for both *35S::HEC1* and *35S::HEC3* (Fig. 6J,K). Both of the latter phenotypes are very similar to what has been reported for the *pin1* mutant (Okada et al., 1991). *PIN1* belongs to the *PIN* family of auxin efflux carriers, which play an important role in setting up auxin gradients or patterns of flow that pattern the plant (Benkova et al., 2003; Friml, 2003; Friml et al., 2003). The overproliferation of stigmatic tissue in *35S::HEC* lines suggests the pooling of auxin or an increased auxin response at these sites. This interesting link between the *HEC* genes and auxin should be investigated in future studies.

In summary, the *HEC* genes function redundantly in patterning tissues crucial for reproductive success in the *Arabidopsis* gynoecium. Elucidating additional details about how the *HECs* interact with other carpel-patterning genes will help to provide insights into various aspects of gynoecium function, including carpel development, pollen tube growth and fertilization.

We thank Yat Long Poon and Nancy Lee for excellent technical assistance in the laboratory; Evelyn York for technical help with SEM work carried out at the Scripps Institution of Oceanography; Adrienne Roeder for many helpful discussions and support throughout the project, and Brian Crawford, Juan Jose Ripoll and Sangho Jeong for carefully reviewing this manuscript. This work is funded by a National Science Foundation grant to M.F.Y.

Supplementary material

Supplementary material for this article is available at http://dev.biologists.org/cgi/content/full/134/20/3593/DC1

References

Alonso, J. M., Stepanova, A. N., Leisse, T. J., Kim, C. J., Chen, H., Shinn, P., Stevenson, D. K., Zimmerman, J., Barajas, P., Cheuk, R. et al. (2003). Genome-wide insertional mutagenesis of Arabidopsis thaliana. *Science* **301**, 653-657.

Alvarez, J. and Smyth, D. R. (2002). Crabs claw and Spatula genes regulate growth and pattern formation during gynoecium development in *Arabidopsis thaliana*. *Int. J. Plant Sci.* **163**, 17-41.

Bacsi, S. G., Reiszporszasz, S. and Hankinson, O. (1995). Orientation of the heterodimeric aryl-hydrocarbon (dioxin) receptor complex on its asymmetric DNA recognition sequence. *Mol. Pharmacol.* **47**, 432-438.

Benkova, E., Michniewicz, M., Sauer, M., Teichmann, T., Seifertova, D., Jurgens, G. and Friml, J. (2003). Local, efflux-dependent auxin gradients as a common module for plant organ formation. *Cell* **115**, 591-602.

Blázquez, M. A., Soowal, L. N., Lee, I. and Weigel, D. (1997). LEAFY expression and flower initiation in *Arabidopsis*. *Development* **124**, 3835-3844.

Crawford, B. C. W., Ditta, G. and Yanofsky, M. F. (2007). The *NTT* Gene is required for transmitting tract development in carpels of *Arabidopsis thaliana*. *Curr. Biol.* **17**, 1101-1108.

Dinneny, J. R., Yadegari, R., Fischer, R. L., Yanofsky, M. F. and Weigel, D. (2004). The role of JAGGED in shaping lateral organs. *Development* **131**, 1101-1110.

Ellenberger, T., Fass, D., Arnaud, M. and Harrison, S. C. (1994). Crystal-structure of transcription factor E47–E-box recognition by a basic region helix-loop-helix dimer. *Genes Dev.* **8**, 970-980.

Ferrandiz, C., Liljegren, S. J. and Yanofsky, M. F. (2000). Negative regulation of the SHATTERPROOF genes by FRUITFULL during *Arabidopsis* fruit development. *Science* **289**, 436-438.

Friml, J. (2003). Auxin transport – shaping the plant. *Curr. Opin. Plant Biol.* **6**, 7-12.

Friml, J., Vieten, A., Sauer, M., Weijers, D., Schwarz, H., Hamann, T., Offringa, R. and Jurgens, G. (2003). Efflux-dependent auxin gradients establish the apical-basal axis of *Arabidopsis*. *Nature* **426**, 147-153.

Gleave, A. P. (1992). A versatile binary vector system with a T-DNA organizational-structure conducive to efficient integration of cloned DNA into the plant genome. *Plant Mol. Biol.* **20**, 1203-1207.

Heim, M. A., Jakoby, M., Werber, M., Martin, C., Weisshaar, B. and Bailey, P. C. (2003). The basic helix-loop-helix transcription factor family in plants: A genome-wide study of protein structure and functional diversity. *Mol. Biol. Evol.* **20**, 735-747.

Heisler, M. G., Atkinson, A., Bylstra, Y. H., Walsh, R. and Smyth, D. R. (2001). SPATULA, a gene that controls development of carpel margin tissues in Arabidopsis, encodes a bHLH protein. *Development* **128**, 1089-1098.

Jiang, L., Yang, S. L., Xie, L. F., Puah, C. S., Zhang, X. Q., Yang, W. C., Sundaresan, V. and Ye, D. (2005). VANGUARD1 encodes a pectin methylesterase that enhances pollen tube growth in the *Arabidopsis* style and transmitting tract. *Plant Cell* **17**, 584-596.

Johnson, M. A. and Preuss, D. (2002). Plotting a course: multiple signals guide pollen tubes to their targets. *Dev. Cell* **2**, 273-281.

Kuusk, S., Sohlberg, J. J., Long, J. A., Fridborg, I. and Sundberg, E. (2002). STY1 and STY2 promote the formation of apical tissues during *Arabidopsis* gynoecium development. *Development* **129**, 4707-4717.

Lennon, K. A., Roy, S., Hepler, P. K. and Lord, E. M. (1998). The structure of the transmitting tissue of *Arabidopsis thaliana* (L.) and the path of pollen tube growth. *Sexual Plant Reprod.* **11**, 49-59.

Liljegren, S. J., Ditta, G. S., Eshed, H. Y., Savidge, B., Bowman, J. L. and Yanofsky, M. F. (2000). SHATTERPROOF MADS-box genes control seed dispersal in Arabidopsis. *Nature* **404**, 766-770.
Liljegren, S. J., Roeder, A. H. K., Kempin, S. A., Gremski, K., Ostergaard, L., Guimil, S., Reyes, D. K. and Yanofsky, M. F. (2004). Control of fruit patterning in *Arabidopsis* by INDEHISCENT. *Cell* **116**, 843-853.
Ma, P. C. M., Rould, M. A., Weintraub, H. and Pabot, C. O. (1994). Crystal structure of MyoD bHLH domain-DNA complex - perspectives on DNA recognition and implications for transcriptional activation. *Cell* **77**, 451-459.
Massari, M. E. and Murre, C. (2000). Helix-loop-helix proteins: regulators of transcription in eucaryotic organisms. *Mol. Cell. Biol.* **20**, 429-440.
Murre, C., Bain, G., Vandijk, M. A., Engel, I., Furnari, B. A., Massari, M. E., Matthews, J. R., Quong, M. W., Rivera, R. R. and Stuiver, M. H. (1994). Structure and function of helix-loop-helix proteins. *Biochim. Biophys. Acta* **1218**, 129-135.
Nemhauser, J. L., Feldman, L. J. and Zambryski, P. C. (2000). Auxin and ETTIN in *Arabidopsis* gynoecium morphogenesis. *Development* **127**, 3877-3888.
Okada, K., Ueda, J., Komaki, M. K., Bell, C. J. and Shimura, Y. (1991). Requirement of the auxin polar transport-system in early stages of *Arabidopsis* floral bud formation. *Plant Cell* **3**, 677-684.
Palanivelu, R. and Preuss, D. (2006). Distinct short-range ovule signals attract or repel Arabidopsis thaliana pollen tubes in vitro. *BMC Plant Biol.* **6**, 7.
Palanivelu, R., Brass, L., Edlund, A. F. and Preuss, D. (2003). Pollen tube growth and guidance is regulated by POP2, an *Arabidopsis* gene that controls GABA levels. *Cell* **114**, 47-59.
Pelaz, S., Gustafson-Brown, C., Kohalmi, S. E., Crosby, W. L. and Yanofsky, M. F. (2001). APETALA1 and SEPALLATA3 interact to promote flower development. *Plant J.* **26**, 385-394.
Rosso, M. G., Li, Y., Strizhov, N., Reiss, B., Dekker, K. and Weisshaar, B. (2003). An *Arabidopsis thaliana* T-DNA mutagenized population (GABI-Kat) for flanking sequence tag-based reverse genetics. *Plant Mol. Biol.* **53**, 247-259.
Scott, J. E. and Dorling, J. (1965). Differential staining of acid glycosaminoglycans (mucopolysaccharides) by Alcian blue in salt solutions. *Histochem. Cell Biol.* **5**, 221-233.
Sessions, R. A. and Zambryski, P. C. (1995). *Arabidopsis* gynoecium structure in the wild and in *ettin* mutants. *Development* **121**, 1519-1532.
Sohlberg, J. J., Myrenas, M., Kuusk, S., Lagercrantz, U., Kowalczyk, M., Sandberg, G. and Sundberg, E. (2006). STY1 regulates auxin biosynthesis and affects apical-basal patterning of the *Arabidopsis* gynoecium. *Plant J.* **47**, 112-123.
Swanson, H. I., Chan, W. K. and Bradfield, C. A. (1995). DNA-binding specificities and pairing rules of the Ah receptor, ARNT, and SIM proteins. *J. Biol. Chem.* **270**, 26292-26302.
Toledo-Ortiz, G., Huq, E. and Quail, P. H. (2003). The Arabidopsis basic/helix-loop-helix transcription factor family. *Plant Cell* **15**, 1749-1770.
Wang, H., Wu, H. M. and Cheung, A.Y. (1996). Pollination induces mRNA poly(A) tail-shortening and cell deterioration in flower transmitting tissue. *Plant J.* **9**, 715-727.
Wesley, S. V., Helliwell, C. A., Smith, N. A., Wang, M. B., Rouse, D. T., Liu, Q., Gooding, P. S., Singh, S. P., Abbott, D., Stoutjesdijk, P. A. et al. (2001). Construct design for efficient, effective and high-throughput gene silencing in plants. *Plant J.* **27**, 581-590.

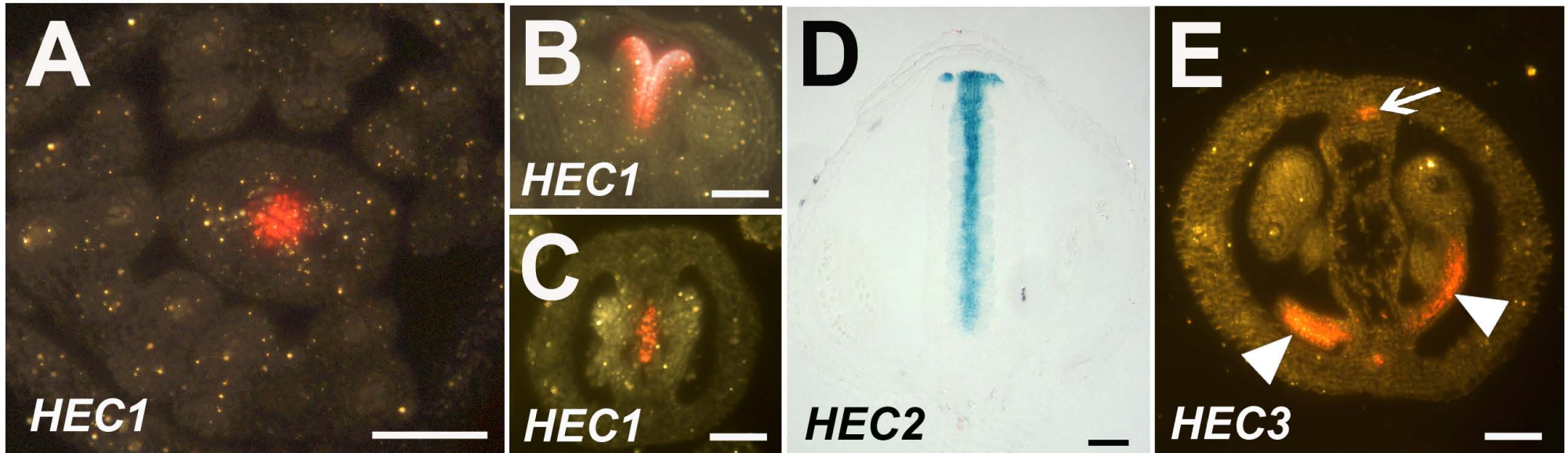
A
HEC1
B
HEC1
C
HEC1
D
HEC2
E
HEC3

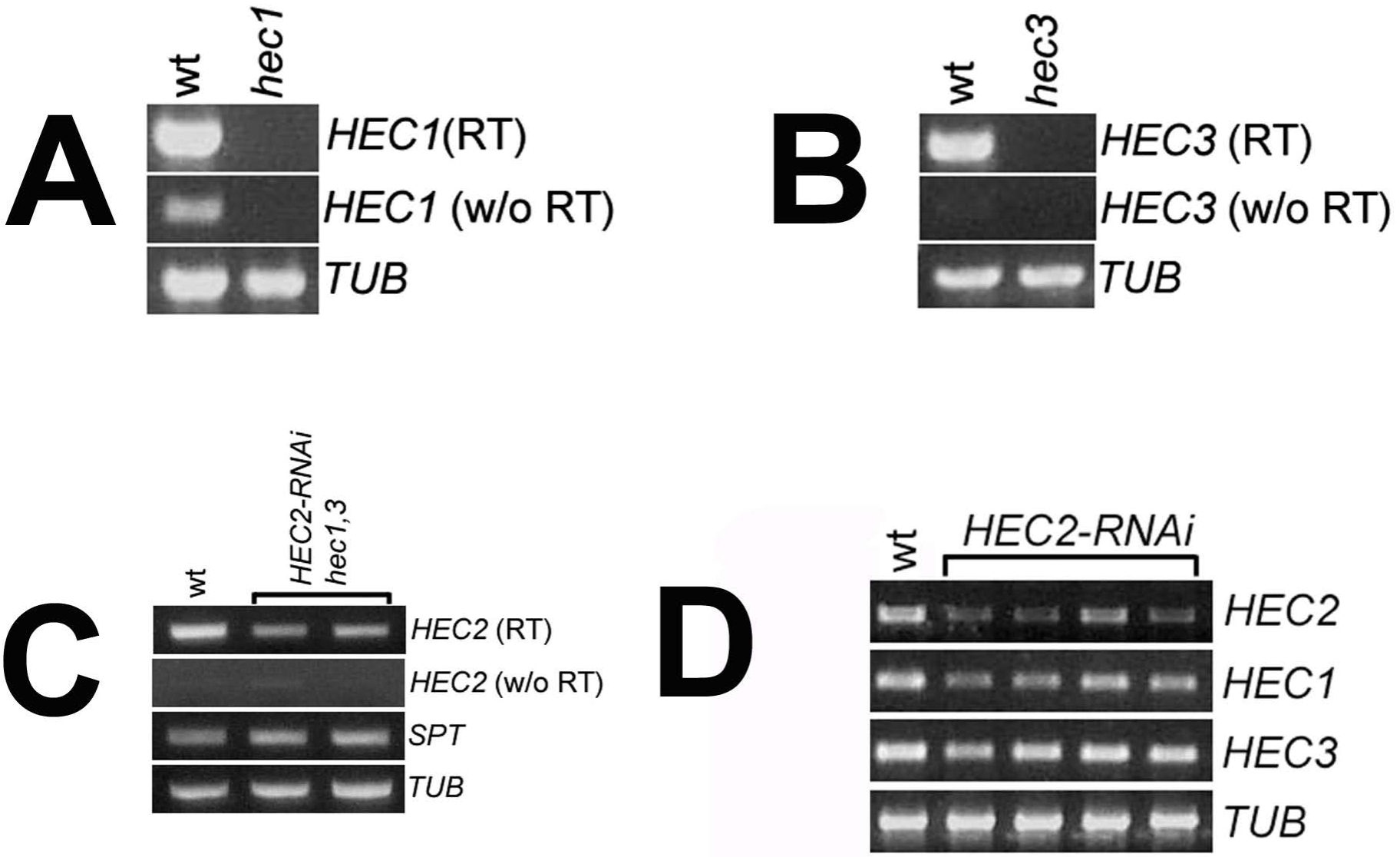
A
wt
hec1
HEC1(RT)
HEC1 (w/o RT)
TUB
B
wt
hec3
HEC3 (RT)
HEC3 (w/o RT)
TUB
C
wt
HEC2-RNAi
hec1,3
HEC2 (RT)
HEC2 (w/o RT)
SPT
TUB
D
wt
HEC2-RNAi
HEC2
HEC1
HEC3
TUB

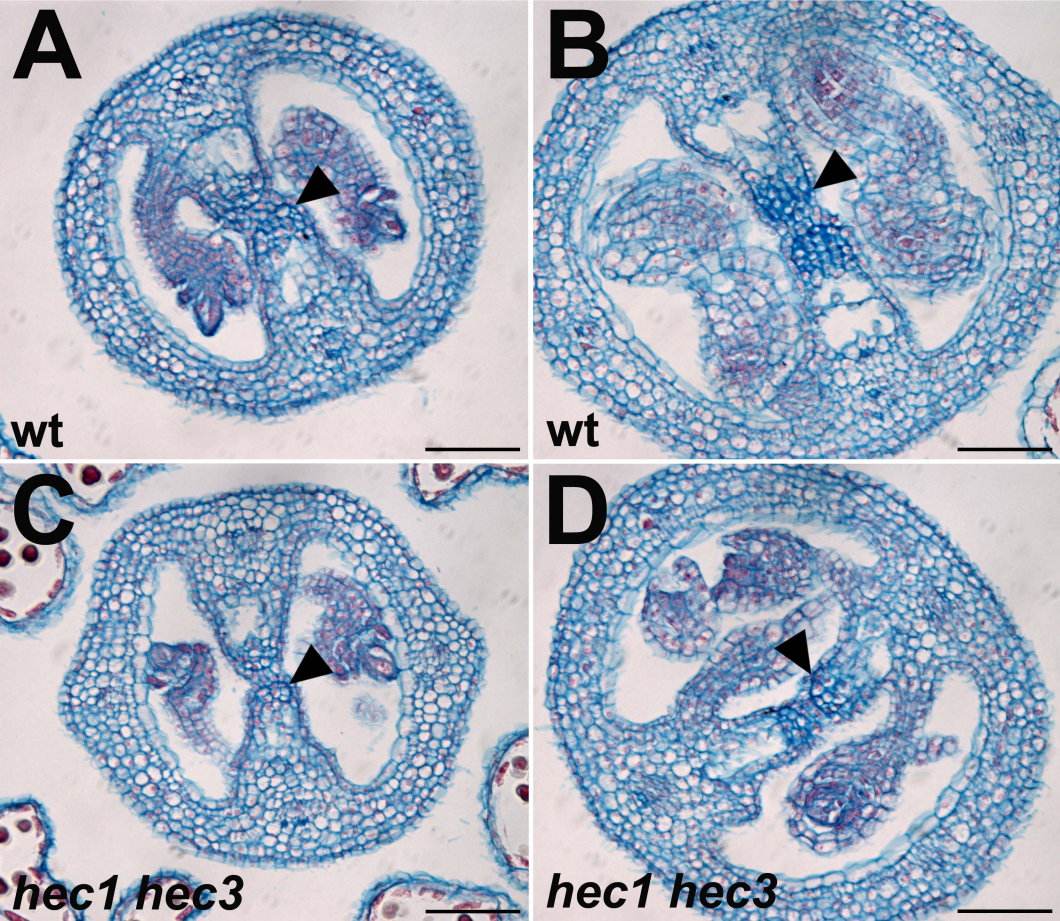
A
wt
B
wt
C
hec1 hec3
D
hec1 hec3